

УДК 621.382

# Implementation of Reading Electronics of Silicone Photomultiplier Tubes on the Array Chip MH2XA030

Dvornikov O. V.<sup>1</sup>, Tchekhovski V. A.<sup>2</sup>, Prokopenko N. N.<sup>3,4</sup>, Galkin Ya. D.<sup>5</sup>, Kunts A. V.<sup>5</sup>, Bugakova A. V.<sup>3</sup>

<sup>1</sup>Public Joint Stock Company “MNIPP”, Belarus

<sup>2</sup>Institute for Nuclear Problems BSU, Belarus

<sup>3</sup>Don State Technical University, Russia; <sup>4</sup>Institute for Design Problems in Microelectronics of RAS, Russia

<sup>5</sup>Belarusian State University of Informatics and Radioelectronics, Belarus

E-mail: [prokopnik1949@gmail.com](mailto:prokopnik1949@gmail.com)

The implementation of a charge-sensitive amplifier (CSA) based on the MH2XA030 array chip (AC) with an adjustable conversion factor for processing signals of silicone photomultipliers (SPM) is considered. The developed CSA, named ADPreamp13, contains a fast and slow signal circuit (SC). The fast SC includes a transresistive amplifier-shaper with a base-level adjustment circuit, and a slow SC includes a CSA, a shaper, and a base-level restorer (BLR) circuit. The main advantage of ADPreamp13 amplifier when used in multichannel integrated circuits is the minimum number of elements used, due to the use of the same stages to perform different functions. To correctly simulate the operation of ADPreamp13, taking into account the features of the input signal source, a simplified electrical equivalent circuit of the SPM, applicable to both circuit simulation and measurements, is proposed. Circuit simulation of ADPreamp13 using the proposed equivalent circuit of SPM with a supply voltage of  $\pm 3$  V, made possible to establish that: fast SC is characterized by the bandwidth up to 60 MHz and allows adjusting the base level in the range from -0.1 V to 0.2 V. Thus, it is possible to compensate the technological variation of the output voltage of the fast SC or set the required switching threshold of the comparator connected to the output of the fast SC; slow SC allows you to adjust the base level in the range from -1 V to 1 V and smoothly change the amplitude of the output signal, including phase inversion, when the control voltage changes from -1 V to 1 V; the BLR circuit provides a constant shape of the output voltage pulse with a DC input current of ADPreamp13, varying in the range of  $\pm 190$   $\mu$ A, and a negligible change of the base level at  $\pm 20\%$  of the resistance variation of integrated resistors. ADPreamp13 amplifier enables the transition to the “sleep” mode with a decrease in current consumption up to 10  $\mu$ A, maintains operability at an absorbed dose of gamma radiation up to 500 krad and the effect of the integral neutron fluence up to  $10^{13}$  n/cm<sup>2</sup> and can be used in multi-channel signal processing chips of SPM.

*Key words:* silicone photomultiplier; readout electronics; array chip; charge-sensitive amplifier

DOI: [10.20535/RADAP.2019.78.60-66](https://doi.org/10.20535/RADAP.2019.78.60-66)

## Introduction

Silicone photomultipliers are successfully used in a number of areas of science and technology for recording various types of electromagnetic emission. Moreover, in a number of products, the use of the SPM has significantly improved technical and economic indicators and transferred the electronic equipment being created to a new qualitative level [1–6].

The analysis of current trends in the design of reading electronics of the SPM allowed us to make an economically sound decision on the creation of reading electronics based on the AC MH2XA030 [7], for the elements of which the CSA circuit was developed.

The purpose of this article is to review the circuit simulation results of the CSA obtained using the proposed SPM model and the previously tested models of the AC elements.

## 1 The Circuit Simulation Results

The ADPreamp13 amplifier circuit developed for the AC MH2XA030 elements is shown in Fig. 1, 2. Fig. 1 illustrates the electrical circuit of the fast and slow signal circuits (SC), and Fig. 2 demonstrates a diagram of the unit for amplification control and base level setting, which provides the operation mode of the ADPreamp13 elements.

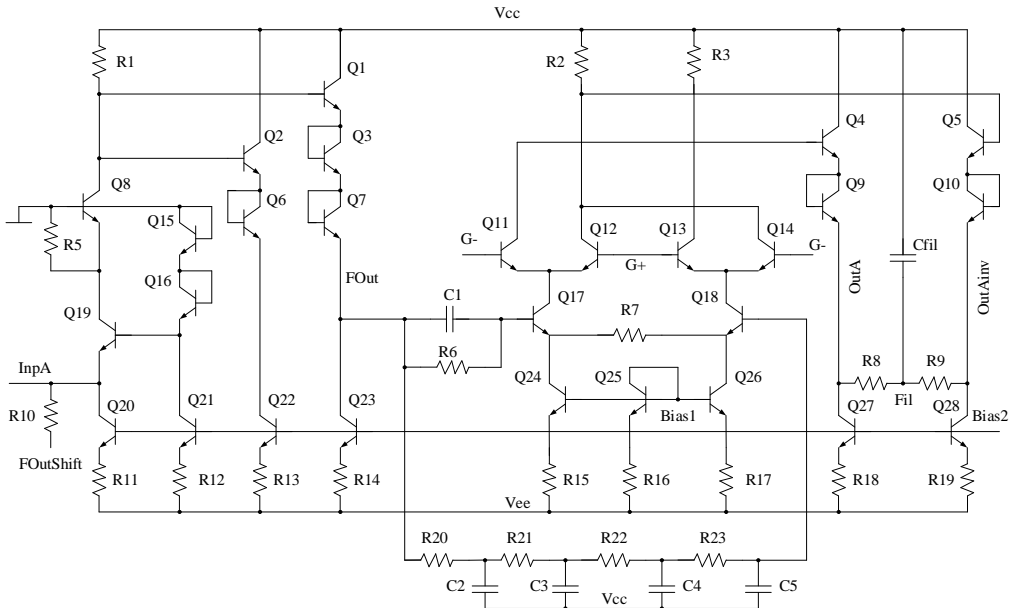


Fig. 1. Electrical circuit of the fast and slow SC of the amplifier ADPreampl3

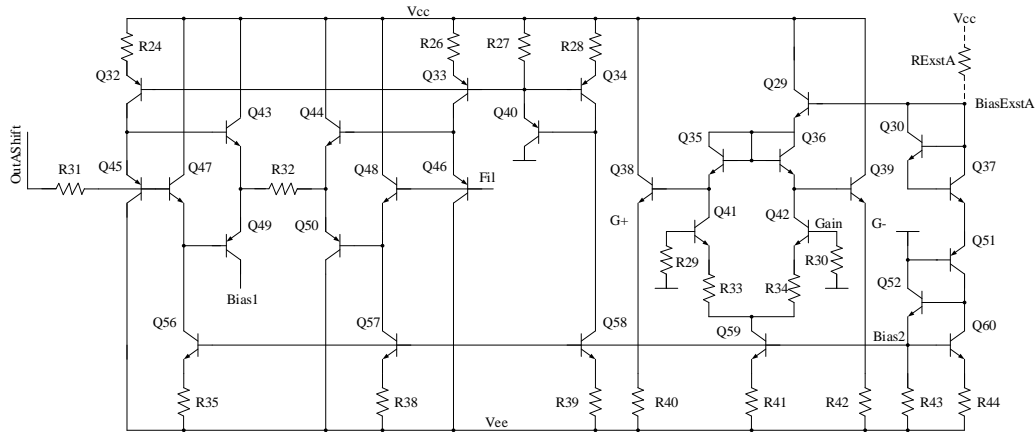


Fig. 2. Electrical circuit of the unit for amplification control and base level setting of the amplifier ADPreampl3

Note that in Fig. 1, 2 all nodes with the same name ( $V_{CC}$ ,  $V_{EE}$ ,  $G^-$ ,  $G^+$ ,  $Bias1$ ,  $Bias2$ ,  $Fil$ ) are interconnected. The purpose of the nodes is the following:  $V_{CC}$ ,  $V_{EE}$  – positive and negative supply voltage; InpA – amplifier input; FOut – fast SC output, OutA, OutAinv – direct and inverse output of the slow SC, FOutShift – voltage setting a base level for the fast SC output, OutAShift – voltage setting a base level for the slow SC outputs, Gain – voltage setting a value of the charge-voltage conversion factor  $K_{QV}$  at the outputs of the slow SC, BiasExtA – resistor that sets the current consumption of the amplifier ( $R_{EXTA} = 15\text{ k}\Omega$  in Fig. 2,  $R_{EXTA} = 1\text{ MOhm}$  – for the “sleep” mode).

The main advantage of the ADPreampl3 amplifier in multi-channel integrated circuits is a minimum number of the elements, due to the use of the same stages to perform different functions. So, the fast SC includes a transresistive amplifier-shaper ( $Q_8, Q_{15}, Q_{16}, Q_{19}, Q_{20}, Q_{21}, R_1, R_5$ ) with an emitter

follower ( $Q_2, Q_6, Q_{22}$ ) and a base level adjustment using resistor  $R_{10}$ , and the slow SC – the same transresistive amplifier-shaper with an emitter follower ( $Q_1, Q_3, Q_7, Q_{23}$ ), differential stage (DC)  $Q_{17}, Q_{18}$  and the BLRC.

As is well known, the correct simulation of the reading electronics implies taking into account the shape of the output signal and the parameters of the SPM [8–12]. In [13, 14], an electrical model of the SPM and a method for identifying its parameters are proposed. The comparison of the results of simulation and measurements of the SPM, connected to the amplifiers of two types, confirming the adequacy of the model, is carried out.

Electrical equivalent circuit of the SPM with SiPM Photonique parameters, containing 516 microcells, is shown in Fig. 3, where: N – number of the switched - charge arising in one microcell when a photon hits; TD, TR, TF, PW, PER, I1, I2 – parameters of a rectangular ideal current source, namely, the time

delay, the rise and fall time, the pulse duration, the period, the initial and final current values, respectively.

Unfortunately, it is difficult to apply the circuit shown in Fig. 3, to simulate an input source when measuring parameters of the reading electronics. We have developed a simplified electrical equivalent circuit of the SPM (Fig. 4), providing at the 50  $\Omega$  load almost the same waveform (Fig. 5), as the circuit of Fig. 3. Moreover, the simulation of the SPM output signal showed that the charge arising in the switched on cells in an amount from 1 to 100 differs for the equivalent circuits of Fig. 3 and Fig. 4 not more than 1.2 %.

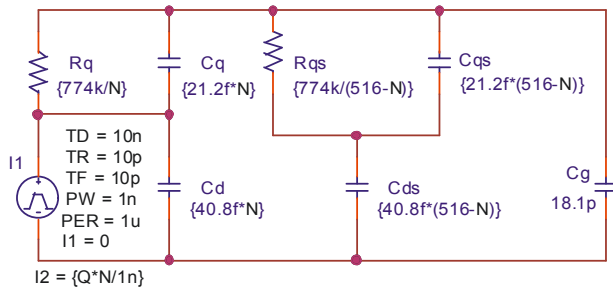


Fig. 3. SiPM Photonique electrical equivalent circuit with 516 microcells [14]

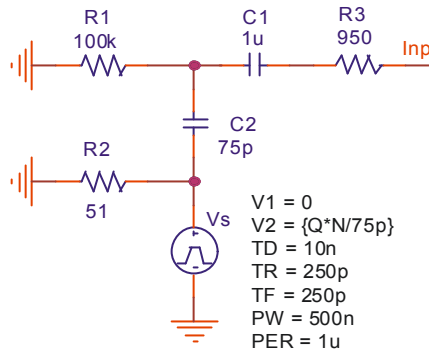


Fig. 4. SiPM Photonique simplified electrical equivalent circuit with 516 microcells

The developed simplified equivalent circuit of the SPM was used in the simulation of the reading electronics and will later be used for measuring the parameters of the manufactured ICs.

In order to adequately evaluate the operation of the ADPreamp13 amplifier in optoelectronic systems, we decided to apply a current signal to the input generated by the simplified electrical circuit of Fig. 4, corresponding to the fixed value of the switched on microcells ( $N = 1, 3, 5, 10, 30, 50, 100$ ), i.e. to the input charge  $Q_{INP} = 127.1 fC * N$ , and to determine the following parameters indicating the equivalent capacitance of the CD signal source:

- peak time  $K_{IV}$  factor for the output of the fast SC, as the ratio of the maximum absolute value of the output voltage to the maximum absolute value of the input current;

- $K_{QV}$  factor for the output of the slow SC, as the ratio of the maximum absolute value of the output voltage to the maximum absolute value of the input charge;
- $T_P$  of the output voltage;
- ranges of permissible parameter adjustments;
- the RMS value of the noise current for the output of the fast SC, referred to the input;
- the RMS value of the noise charge for the output of the slow SC referred to the input;

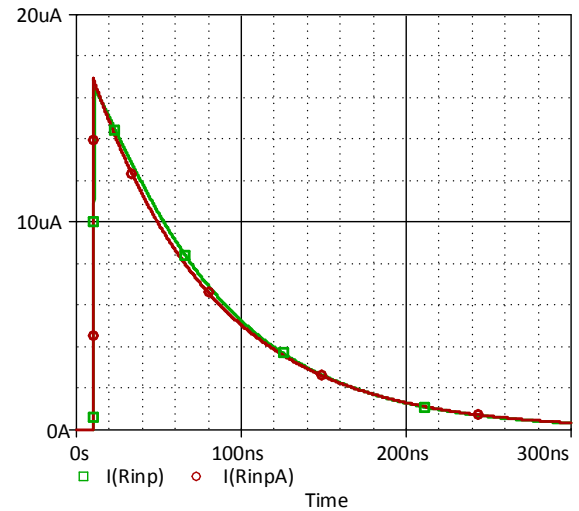


Fig. 5. Simulation results of the SiPM Photonique output signal for 10 switched on microcells:  $I(R_{INP})$  – current flowing through the load resistance in the circuit of Fig. 3,  $I(R_{INPA})$  – current flowing through the load resistance in the circuit of Fig. 4.  $R_{INP} = R_{INPA} = 50 \Omega$

Fig. 6 – 10 and the table 1 show the main simulation results.

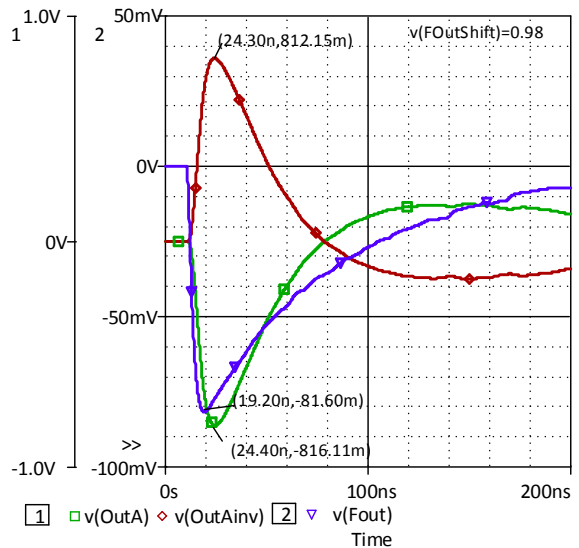


Fig. 6. Voltage pulses at the amplifier outputs for 10 switched on SPM microcells ( $Q_{INP} = 1.271 pC$ ) with  $V_{FOUTSHIFT} = 0.98 V$

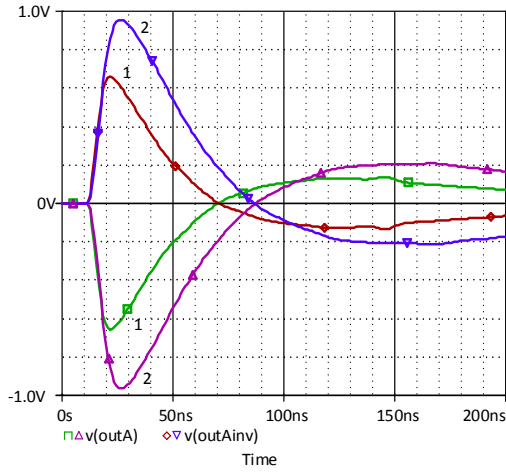


Fig. 7. Voltage pulses at the outputs of the OutA and OutAinv amplifier with  $Q_{INP} = 1.271 \text{ pC}$  and the variation of the resistances of the resistors: 1 –  $0.8R$ ; 2 –  $1.2R$

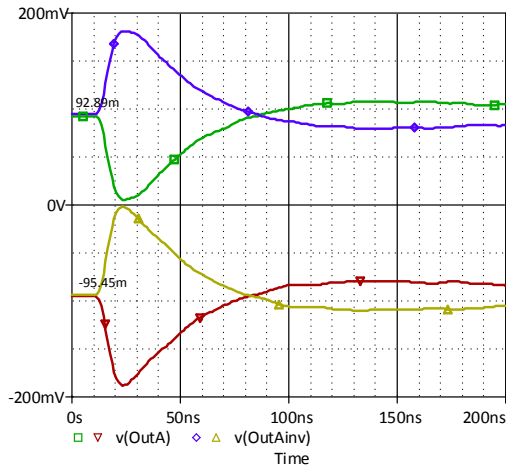


Fig. 8. Voltage pulses at the outputs of the OutA and OutAinv amplifier with  $Q_{INP} = 0.1271 \text{ pC}$ : at the top  $V_{OUTSHIFT} = -0.1 \text{ V}$ ; at the bottom  $V_{OUTSHIFT} = 0.1 \text{ V}$

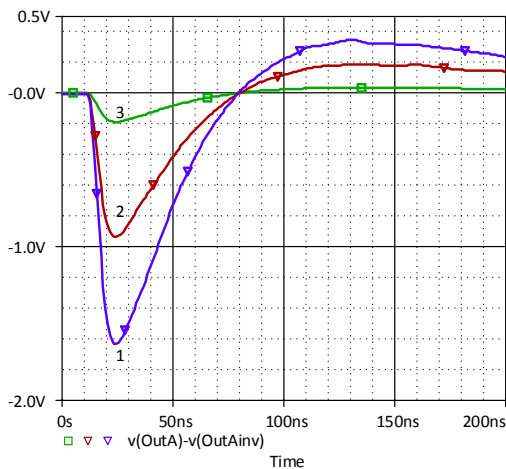


Fig. 9. Voltage pulses between the outputs of the OutA and OutAinv amplifier with  $Q_{INP} = 1.271 \text{ pC}$  and different control voltage: 1 –  $V (\text{Gain}) = 1 \text{ V}$ ; 2 –  $V (\text{Gain}) = 0.5 \text{ V}$ ; 3 –  $V (\text{Gain}) = 0.1 \text{ V}$

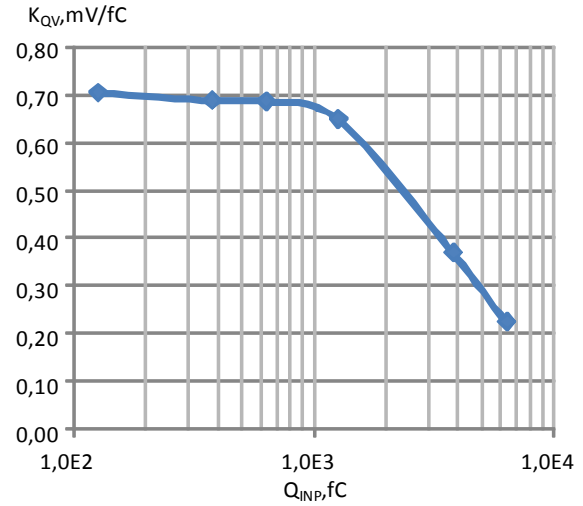


Fig. 10. Dependence of the maximum value of the  $K_{QV}$  conversion factor at the OutA output on the value of the  $Q_{INP}$  input charge at  $C_D \approx 18 \text{ pF}$

Table 1 The main parameters of the amplifier ADPreamp13 when the supply voltage is equal to  $\pm 3 \text{ V}$ , and  $R_{EXTA} = 15 \text{ k}\Omega$

Name of the parameter	Value
Current consumption in idle mode, $\text{mA}$	5.71
Input impedance, $\Omega$	25
$K_{IV}$ conversion factor at $C_D \approx 18 \text{ pF}$ , $\text{mV}/\mu\text{A}$	4.78
The maximum value of the conversion factor $K_{QV}$ at $C_D \approx 18 \text{ pF}$ , $\text{mV}/\text{fC}$	0.7
Base level adjustment range for the OutA outputs (OutInvA), V	$\pm 1$
Base level adjustment range for the FOut output, V	from -0.1 to 0.2
The peak time at the OutA/OutInvA outputs at $C_D \approx 18 \text{ pF}$ , $Q_{INP} \approx 1.3 \text{ pC}$ , ns	14.5/13.5
The peak time at the FOut output at $C_D \approx 18 \text{ pF}$ , $Q_{INP} \approx 1.3 \text{ pC}$ , ns	8.5
-3 dB bandwidth for the OutA (OutInvA) output at $C_D \approx 18 \text{ pF}$ , MHz	from 2.55 to 36.81
-3 dB bandwidth for the FOut output, MHz	from 0 to 60.7
The RMS value of the noise current for the FOut output, referred to the input at $C_D \approx 18 \text{ pF}$ , $\mu\text{A}$	1.11
The RMS value of the noise charge for the OutA output, referred to the input at $C_D \approx 18 \text{ pF}$ , $\text{fC}$	77.16

The performed simulation showed that:

- a voltage change in the FOutShift node within the range from  $-3 \text{ V}$  to  $3 \text{ V}$  causes a change in the level of the DC voltage  $V (FOut)$  at the output of the fast SC from  $0.2 \text{ V}$  to  $-0.1 \text{ V}$ , and  $V (FOut) \approx 0$  with  $V (FOutShift) = 0.98 \text{ V}$

(Fig. 6). Thus, it is possible to compensate for the technological variation of  $V$  (FOut) or to set the required switching threshold of a comparator of the fast SC when one of its inputs is connected to the zero voltage bus, and the second one is connected to  $FOut$ ;

- the BLR provides a constant voltage pulse shape at the OutA, OutAinv outputs with a DC input current of the amplifier varying within the range of  $\pm 190 \mu A$ , a negligible change in the base level, but a noticeable change in the shape of the output pulse of the slow SC at  $\pm 20\%$  variation of the resistances of the integrated resistors (Fig. 7), although the voltage at the FOut output with the specified variation of the resistors changes from 208.1 mV to -170.2 mV;
- when the external  $R_{EXTA}$  resistor is disconnected between the BiasExtA node and the  $V_{CC}$  power supply bus, the amplifier goes into sleep mode and its current consumption from the negative power supply decreases from 5.86 mA to 10  $\mu A$ ;
- the amplifier retains its parameters at the absorbed dose of gamma emission up to 500 krad and the effect of the integrated neutron fluence up to  $10^{13} \text{ n/cm}^2$ ;
- the BLR allows us to smoothly change the base level at the OutA, OutAinv outputs using the voltage at the OutAShift node (Fig. 8). When the supply voltage is equal to  $\pm 3 \text{ V}$ , the recommended shift should not exceed  $\pm 1 \text{ V}$ ;
- in the developed amplifier, the amplitude of the output signal (Fig. 9), including phase inversion, is smoothly adjustable when the voltage  $V$  (Gain) in the Gain node changes from -1 V to 1 V;
- despite the relatively high RMS values of the noise current (1.11  $\mu A$ ) and the noise charge (77.16 fC), the amplifier must provide the registration of two photons using SiPM Photonique, for which the maximum value of the current is 3.4  $\mu A$ , and of the charge - 254.2 fC, i.e. signal-to-noise ratio will be about 3.3.

## Conclusion

For the AC MH2XA030 elements, an ADPreamp13 amplifier has been developed, containing a fast signal circuit and a slow one for signal processing of the SPM.

The fast signal circuit includes a transresistive amplifier-shaper with a bandwidth of up to 60 MHz, a base level trimming circuit in the range from -0.1 V to 0.2 V, and a slow signal circuit – a charge-sensitive amplifier-shaper with a circuit for restoring

and adjusting the base level within the recommended range from -1 V to 1 V and the possibility of electronic adjustment of the conversion factor.

The circuit for restoring and adjusting the base level provides a constant shape of the output voltage pulse at the DC input current of the amplifier, varying within the range of  $\pm 190 \mu A$ , and a negligible change in the base level at  $\pm 20\%$  variation of the resistances of the integrated resistors.

The ADPreamp13 amplifier enables to transfer to the “sleep” mode with a decrease in current consumption up to 10  $\mu A$ , ensures safe operation with an absorbed dose of gamma emission up to 500 krad and the effect of the integrated neutron fluence up to  $10^{13} \text{ n/cm}^2$  and can be used in multi-channel signal processing chips of the SPM.

## Acknowledgments

The research is carried out at the expense of the Grant of the Russian Science Foundation (project № 16-19-00122-P).

## References

- [1] Dvornikov O.V., Tchekhovski V.A., Dyatlov V.L. and Prokopenko N.N. (2014) An integrated circuit for silicon photomultipliers tubes. *Instruments and Experimental Techniques*, Vol. 57, Iss. 1, pp. 40-44. DOI: 10.1134/s0020441214010047
- [2] Dey S., Rudell J.C., Lewellen T.K. and Miyaoka R.S. (2017) A CMOS front-end interface ASIC for SiPM-based positron emission tomography imaging systems. *2017 IEEE Biomedical Circuits and Systems Conference (BioCAS)*. DOI: 10.1109/biocas.2017.8325059
- [3] Cervi T., Babicz M., Bonesini M., Falcone A., Menegolli A., Raselli G.L., Rossella M. and Torti M. (2018) Characterization of SiPM arrays in different series and parallel configurations. *Nuclear Instruments and Methods in Physics Research Section A: Accelerators, Spectrometers, Detectors and Associated Equipment*, Vol. 912, , pp. 209-212. DOI: 10.1016/j.nima.2017.11.038
- [4] Du J., Yang Y., Bai X., Judenhofer M.S., Berg E., Di K., Buckley S., Jackson C. and Cherry S.R. (2016) Characterization of Large-Area SiPM Array for PET Applications. *IEEE Transactions on Nuclear Science*, Vol. 63, Iss. 1, pp. 8-16. DOI: 10.1109/tns.2015.2499726
- [5] Gola A., Acerbi F., Capasso M., Marcante M., Mazzi A., Paternoster G., Piemonte C., Regazzoni V. and Zorzi N. (2019) NUV-Sensitive Silicon Photomultiplier Technologies Developed at Fondazione Bruno Kessler. *Sensors*, Vol. 19, Iss. 2, pp. 308. DOI: 10.3390/s19020308
- [6] Thiessen J.D., Jackson C., O'Neill K., Bishop D., Kozlowski P., Retière F., Shams E., Stortz G., Thompson C.J. and Goertzen A.L. (2013) Performance evaluation of SensL SiPM arrays for high-resolution PET. *2013 IEEE Nuclear Science Symposium and Medical Imaging Conference (2013 NSS/MIC)*, . DOI: 10.1109/nssmic.2013.6829318

- [7] Dvornikov O., Tchekhovski V., Dziatlau V., Prokopenko N. and Butyrlagin N. (2018) Design of low-temperature DDOAs on the elements of BiJFet array chip MH2XA030. *Serbian Journal of Electrical Engineering*, Vol. 15, Iss. 2, pp. 233-247. DOI: 10.2298/sjee1802233d
- [8] Dvornikov O.V., Tchekhovski V.A., Dyatlov V.L. and Prokopenko N.N. (2014) An integrated circuit for silicon photomultipliers tubes. *Instruments and Experimental Techniques*, Vol. 57, Iss. 1, pp. 40-44. DOI: 10.1134/s0020441214010047
- [9] Villa F., Zou Y., Mora A.D., Tosi A. and Zappa F. (2015) SPICE Electrical Models and Simulations of Silicon Photomultipliers. *IEEE Transactions on Nuclear Science*, Vol. 62, Iss. 5, pp. 1950-1960. DOI: 10.1109/tns.2015.2477716
- [10] Marano D., Bonanno G., Garozzo S., Romeo G., Grasso A.D., Palumbo G. and Pennisi S. (2015) A new enhanced PSPICE implementation of the equivalent circuit model of SiPM detectors. *2015 IEEE 13th International New Circuits and Systems Conference (NEWCAS)*. DOI: 10.1109/newcas.2015.7182010
- [11] Bagliesi M., Avanzini C., Bigongiari G., Cecchi R., Kim M., Maestro P., Marrocchesi P. and Morsani F. (2011) A custom front-end ASIC for the readout and timing of 64 SiPM photosensors. *Nuclear Physics B - Proceedings Supplements*, Vol. 215, Iss. 1, pp. 344-348. DOI: 10.1016/j.nuclphysbps.2011.04.049
- [12] Przyborowski D., Kaplon J. and Rymaszewski P. (2016) Design and Performance of the BCM1F Front End ASIC for the Beam Condition Monitoring System at the CMS Experiment. *IEEE Transactions on Nuclear Science*, Vol. 63, Iss. 4, pp. 2300-2308. DOI: 10.1109/tns.2016.2575781
- [13] Corsi F., Foresta M., Marzocca C., Matarrese G. and Guerra A.D. (2009) ASIC development for SiPM readout. *Journal of Instrumentation*, Vol. 4, Iss. 03, pp. P03004-P03004. DOI: 10.1088/1748-0221/4/03/p03004
- [14] Corsi F., Dragone A., Marzocca C., Guerra A.D., Delizia P., Dinu N., Piemonte C., Boscardin M. and Betta G.D. (2007) Modelling a silicon photomultiplier (SiPM) as a signal source for optimum front-end design. *Nuclear Instruments and Methods in Physics Research Section A: Accelerators, Spectrometers, Detectors and Associated Equipment*, Vol. 572, Iss. 1, pp. 416-418. DOI: 10.1016/j.nima.2006.10.219

## Реалізація зчитуючої електроніки кремнієвих фотоелектронних помножувачів на базовому матричному кристалі MH2XA030

*Дворніков О. В., Человський В. О.,  
Прокопенко М. М., Галкін Я. Д., Кунц О. В.,  
Бугакова Г. В.*

Розглянута реалізація на базовому матричному кристалі MH2XA030 зарядочутливого підсилювача (ЗЧП) з регульованим коефіцієнтом перетворення, призначеного для обробки сигналів кремнієвих фотоелектронних помножувачів (SiФЕП). Розроблений ЗЧП, названий ADPreampl3, містить швидке і повільне сигнальне коло (СК). Швидке СК включає трансрезистивний підсилювач-формувавч зі схемою підстроювання базового рівня, а повільне СК - ЗЧУ, формувавч, схему відновлення базового рівня (ВБР). Головною перевагою

підсилювача ADPreampl3 у разі його застосування в багатоканальних ІС є мінімальна кількість використовуваних елементів, що обумовлено застосуванням одних і тих же каскадів для виконання різних функцій. Для коректного моделювання роботи ADPreampl3 з урахуванням особливостей джерела вхідного сигналу запропонована спрощена електрична еквівалентна схема SiФЕП, що використовується як для схематичного моделювання, так і для вимірювань. Схематичне моделювання ADPreampl3 з використанням запропонованої еквівалентної схеми SiФЕП у разі, якщо напруга джерела живлення дорівнює  $\pm 3$  В, дозволило встановити, що:

- швидке СК характеризується пропускнуою здатністю до 60 МГц і дозволяє підлаштовувати базовий рівень в діапазоні від -0,1 В до 0,2 В. Таким чином можлива компенсація технологічного розкиду вихідної напруги швидкого СК або установки необхідного порогу перемикання компаратора, що підключається до виходу швидкого СК;

- повільне СК дозволяє регулювати базовий рівень в діапазоні від -1 В до 1 В і плавно змінювати амплітуду вихідного сигналу, включаючи інверсію фази, у разі зміни керуючої напруги від -1 В до 1 В;

- схема ВБР забезпечує незмінну форму вихідного імпульсу напруги при постійному вхідному струмі ADPreampl3, що змінюється в діапазоні  $\pm 190$  мкА, і пренебрежимо малу зміну базового рівня у разі  $\pm 20\%$  відхилення значень опорів інтегральних резисторів.

Підсилювач ADPreampl3 допускає перехід в "сплячий" режим зі зменшенням струму споживання до 10 мкА, зберігає працездатність при поглиненні дозі гамма-випромінювання до 500 крад і впливі інтегрального потоку нейтронів до  $10^{13}$  н/см<sup>2</sup> і може знайти застосування в багатоканальних мікросхемах обробки сигналів SiФЕП.

*Ключові слова:* кремнієвий фотоелектронний помножувач; зчитуюча електроніка; базовий матричний кристал; зарядочутливий підсилювач

## Реализация считывающей электроники кремниевых фотоэлектронных умножителей на базовом матричном кристалле MH2XA030

*Дворников О. В., Человский В. А.,  
Прокопенко М. М., Галкин Я. Д., Кунц О. В.,  
Бугакова Г. В.*

Рассмотрена реализация на базовом матричном кристалле MH2XA030 зарядочувствительного усилителя (ЗЧУ) с регулируемым коэффициентом преобразования, предназначенного для обработки сигналов кремниевых фотоэлектронных умножителей (SiФЭУ).

Разработанный ЗЧУ, названный ADPreampl3, содержит быструю и медленную сигнальную цепь (СЦ). Быстрая СЦ включает трансрезистивный усилитель-формирователь со схемой подстройки базового уровня, а медленная СЦ — ЗЧУ, формирователь, схему восстановления базового уровня (ВБУ). Главным преимуществом усилителя ADPreampl3 при его применении в многоканальных ИС является минимальное количество используемых элементов, обусловленное применением одних и тех же каскадов для выполнения разных функций. Для

корректного моделирования работы ADPreamp13 с учетом особенностей источника входного сигнала предложена упрощенная электрическая эквивалентная схема SiФЭУ, применимая как для схемотехнического моделирования, так и для измерений. Схемотехническое моделирование ADPreamp13 с использованием предложенной эквивалентной схемы SiФЭУ при напряжении источников питания, равном  $\pm 3$  В, позволило установить, что:

- быстрая СЦ характеризуется полосой пропускания до 60 МГц и позволяет подстраивать базовый уровень в диапазоне от -0,1 В до 0,2 В. Таким образом возможна компенсация технологического разброса выходного напряжения быстрой СЦ или установка требуемого порога переключения компаратора, подключаемого к выходу быстрой СЦ;

- медленная СЦ позволяет регулировать базовый уровень в диапазоне от -1 В до 1 В и плавно изменять амплитуду выходного сигнала, включая инверсию фа-

зы, при изменении управляющего напряжения от -1 В до 1 В;

- схема ВБУ обеспечивает неизменную форму выходного импульса напряжения при постоянном входном токе ADPreamp13, изменяющемся в диапазоне  $\pm 190$  мкА, и пренебрежимо малое изменение базового уровня при  $\pm 20\%$  разбросе сопротивлений интегральных резисторов.

Усилитель ADPreamp13 допускает переход в “спящий” режим с уменьшением тока потребления до 10 мкА, сохраняет работоспособность при поглощенной дозе гамма-излучения до 500 крэд и воздействии интегрального потока нейтронов до  $10^{13}$  н/см<sup>2</sup> и может найти применение в многоканальных микросхемах обработки сигналов SiФЭУ.

*Ключевые слова:* кремниевый фотоэлектронный умножитель; считывающая электроника; базовый матричный кристалл; зарядочувствительный усилитель